Results in Materials 7 (2020) 100099

Contents lists available at ScienceDirect

Results in Materials

journal homepage: www.journals.elsevier.com/results-in-materials

Synthesis and characterization of zinc and copper oxide nanoparticles and their antibacteria activity

R.B. Asamoah [a], A. Yaya [a], B. Mensah [a], P. Nbalayim [a], V. Apalangya [b], Y.D. Bensah [a], L.N.W. Damoah [a], B. Agyei-Tuffour [a], D. Dodoo-Arhin [a], E. Annan [a,*]

[a] Department of Materials Science and Engineering, School of Engineering Sciences, CBAS, University of Ghana, Legon, Ghana
[b] Department of Food Process Engineering, School of Engineering Sciences, CBAS, University of Ghana, Legon, Ghana

ARTICLE INFO

Keywords:
Antibacteria
Nanoparticles
Disk diffusion test
Optical density test

ABSTRACT

Inorganic nano-metal oxides can be effective alternatives to drug resistant organic antibiotics due to their broad spectrum antimicrobial activity against pathogenic and mutagenic gram-negative and positive bacteria. In this study, zinc and copper oxides (ZnO and CuO) were synthesised using a wet chemical reduction method. The oxide nanoparticles were characterized using X-ray diffraction (XRD), UV–Vis spectrometer, Fourier Transformed Infrared spectrometer and Transmission electron microscopy (TEM). The antibacterial activities of the nanoparticles were investigated against *e. coli* and *s. aureus* using disk diffusion and microdilution tests. The TEM micrographs showed that copper oxide nanoparticles assumed a nanorod shape of average length of 100 nm whiles zinc oxide nanoparticles were spherical of average diameter of 15 nm. The FTIR results showed that the nanoparticles were free of impurities and organic surfactants, which was confirmed by XRD. For the antibacteria tests, the minimum inhibition concentration (MIC) of CuO against *e. coli* and *s. aureus* were 1 mg/ml and 0.25 mg/ml respectively whiles it was 0.1 mg/ml for ZnO against *s. aureus* with ZnO producing no inhibition against *e. coli*. With the microdilution test, both nanoparticles exhibited activity against both bacterias at all varying concentrations. The results concluded that CuO had higher antibacteria activity compared to ZnO.

1. Introduction

The incidence of antibiotic resistive pathogens has led to the continuous search for new alternatives [1]. Among drug resistive pathogens, water borne bacteria species pose a real threat to public health as they are responsible for the outbreak of diseases such as diarrhoea which accounts for 2195 global infant mortality per day [2].

Inorganic nanoparticles have demonstrated toxicity against a wide range of pathogenic bacterial species [3]. Even though, the broad-spectrum biocidal effect of inorganic nanomaterials are well known, the bacteriocidal effect is poorly understood [4]. It has been proposed that the release of ions into solution creates reactive oxygen species which is toxic to bacteria. Other studies showed that nanoparticles by virtue of their size can penetrate bacterial cell walls and attack organelles which leads to cell death [5]. Unlike organic antibiotics, the inorganic counterparts have multi-targeting pathways to combat drug resistive pathogens through mutations [6].

Among inorganic nanoparticles, metal oxide nanoparticles are widely considered for their antibacteria activities [7]. This is mostly attributed to the fact that metal oxides have easy synthesis routes which can be controlled to tune the size and shape of the nanoparticles and they are also cheaper as compared to metal nanoparticles such as silver and gold [8]. Copper and zinc oxides are considered as suitable alternatives to organic based antimicrobials. Their antibacteria effect is dependent on a number of factors which are mostly determined by the method of synthesis [1]. These factors include their size, the presence of surfactant, their shape and other factors [9]. Metal nanoparticles, due to their small size and high reactivity easily diffuse through the well wall of bacteria to attach themselves to internal proteins and organelles leading to bacteria death [10,11]. The activities of nanoparticles is also affected by the presence of surfactants on their surfaces. Whiles certain surfactants enhance cell growth, others inhibit cell growth and may event cause cell death. The synthesis of nanoparticles with certain surfactant will result in the respective effect of promoting or impeding cell proliferation [12] For

* Corresponding author.
E-mail addresses: rbasamoah001@st.ug.edu.gh (R.B. Asamoah), ayaya@ug.edu.gh (A. Yaya), bismarkmensah@ug.edu.gh (B. Mensah), sugril2002@yahoo.com (P. Nbalayim), vapangya@ug.edu.gh (V. Apalangya), ydbensah@ug.edu.gh (Y.D. Bensah), lnwdamoah@ug.edu.gh (L.N.W. Damoah), bagyei-tuffour@ug.edu.gh (B. Agyei-Tuffour), ddodoo-arhin@ug.edu.gh (D. Dodoo-Arhin), ebannan@ug.edu.gh (E. Annan).

https://doi.org/10.1016/j.rinma.2020.100099
Received in revised form 17 March 2020; Accepted 2 April 2020
Available online 30 May 2020

instance, the cationic surfactant; cetyltrimethylammonium bromide (CTAB) is reported to possess antibacteria activity [13].The shape of nanoparticles can influences its toxicity [9]. Cubic silver nanoparticles were found to be more toxic than its spherical counterpart [14]. Among many reasons, this may be chiefly due to their respective release of ionic species in solution which is the major antibacteria agent. Also, the nanoparticle's diffusive rate through the pores of cell walls [15]. The permeability of nanoparticles through cell walls is related to the particle size and shape [16]. Therefore, these physical properties of nanoparticles dictate their characteristics which affect their application including antibacteria use. In particular, the antibacteria application is highly reliant upon the ability of the nanoparticle to release ions into solution. Also, its ability to pass through cellular pores to disrupt organelles [17]. A host of synthesis methods and parameters can be adopted to realise specific features of nanoparticles [18]. Among them the wet-chemical method is frequently used due to its simplicity and cost effectiveness [19].

Both copper oxide and zinc oxide have shown varying antibacteria activity against bacteria species [20].They have been used in food packaging, wound healing and surface coatings due to their antimicrobial activities [19,21]. However the antibacteria activities of these nanomaterials are yet to be compared against gram positive and gram negative bacteria species. In this study, investigation into the antibacteria activity on both gram negative and gram positive bacteria using copper oxide and zinc oxide nanoparticles are undertaken. The investigation will compare their respective antibacteria activity against *escherichia coli* (*e. coli*) and *staphylococcus aureus* (*s. aureus)* which are respective gram positive and gram-negative bacteria species. The copper and zinc oxides were synthesised by wet chemical method ensuring surfactant free nanoparticles to eliminate possible influences of surfactants on antibacteria activities.

2. Experimental

2.1. Synthesis of metal oxide nanoparticles

All chemicals were of analytical grade. Copper acetate (copper (II) acetate dihydrate) and zinc acetate (zinc acetate dihydrate) were used as precursors. Sodium hydroxide (grade) was used as the precipitating reagent. All chemicals were purchased from Sigma Aldrich, All aqueous solutions in the synthesis were prepared with deionised water from MilliQ (Milli-Q Water Systems, USA). The synthesis of nanometal oxide particles (metal oxide nanoparticles) was carried out by the facile wet chemical precipitation method. The wet chemical precipitation synthesis method convertes respective ionic solution into their insoluble nanometal oxide precipitates with the aid of a precipitating reagent. Pure crystalline powdered nanometal oxides are obtained by separating precipitates from solution, drying and also calcination.

The following chemical equations describes the formation of nanometal oxides by the wet chemical synthesis:

$$(\boldsymbol{M}(\boldsymbol{CH_2COO})\boldsymbol{aq} \rightleftharpoons \boldsymbol{M}^{+} + \boldsymbol{CH_2COO}^{-} \quad (1)$$

$$\boldsymbol{M}^{+} + \boldsymbol{NaOH} \rightarrow \boldsymbol{MOH} \quad (2)$$

$$\mathbf{MOH} \rightleftharpoons \boldsymbol{MO} + \boldsymbol{H}_2 0 \quad (3)$$

where in equation (1), ionic species M^+ is formed from the dissociation of $(\boldsymbol{M}(\boldsymbol{CH_2COO})$. NaOH in equation (2) is the precipitating reagent. MO which is a nanometal oxide is formed in 3. M is the metal component of the salt $(\boldsymbol{M}(\boldsymbol{CH_2COO})$.

2.2. Synthesis of copper oxide nanoparticles

0.1 M copper acetate was dissolved in 100 ml of deionised water. The solution was continuously stirred at 700 rpm on a magnetic stirrer hot plate at 80 °C (H4000-HS, Benchmark Scientific, USA). The homogenous solution pH was adjusted to 11 with 2 M NaOH. The solution was continuously stirred at same speed and temperature for another 60 min. A black suspension with precipitates was formed, which is indicative of the formation of copper oxide (A [7]. The temperature was allowed to gradually cool to room temperature at the same continuous stirring speed. The precipitates were separated by centrifugation and washed several times with distilled water to remove excess ions. The particles obtained were dried in an oven at 80 °C overnight. It was the then calcined at 500 °C to remove impurities which may be present on particles surfaces. The particles were subsequently characterized and applied for antibacteria activities. The formation of copper oxide nanoparticles is as described by the following chemical reactions 4–6:

$$\left(\boldsymbol{Cu}(\boldsymbol{CH_2COO})_2\right)\boldsymbol{aq} \rightleftharpoons \boldsymbol{Cu}^{2+} + \boldsymbol{CH_2COO}^{-} \quad (4)$$

$$\boldsymbol{Cu}^{2+} + \boldsymbol{NaOH} \rightleftharpoons \boldsymbol{Cu}(\boldsymbol{OH})_2 \quad (5)$$

$$\boldsymbol{Cu}(\boldsymbol{OH})_2 \rightleftharpoons \boldsymbol{CuO}_2 + \boldsymbol{H}_2 0 \quad (6)$$

2.3. Synthesis of zinc oxide nanoparticles

Similarly, 0.1 M zinc acetate was dissolved in 100 rpm of deionised water. A homogeneous solution was obtained after keeping the solution at 700 rpm on a hot magnetic stirrer plate (H4000-HS, Benchmark Scientific, USA) at 80 °C. The temperature and stirring speed were kept constant throughout the synthesis period. A 2 M NaOH was added to the homogeneous solution to increase its pH to 11. A white precipitate was formed. The synthesis was allowed to continue for another 60 min. The precipitates were separated by centrifugation at 6000 rpm. The particles were severally washed to remove unreacted ions. They were dried at 80 °C for overnight and further calcined at 500 °C for 3 h at a heating rate of 1 °C/S. The synthesised particles were successively analysed through a series of characterizations and utilized for antibiotic studies. The reactions that leads to the formation of zinc oxide nanoparticles is as described by equations (7)–(9);

$$\left(\boldsymbol{Zn}(\boldsymbol{COO})_2\right)\boldsymbol{aq} \rightleftharpoons \boldsymbol{Zn}^{2+} + \boldsymbol{CH_2COO}^{-} \quad (7)$$

$$\boldsymbol{Zn}^{2+} + \boldsymbol{NaOH} \rightleftharpoons \boldsymbol{Zn}(\boldsymbol{OH})_2 \quad (8)$$

$$\boldsymbol{Zn}(\boldsymbol{OH})_2 \rightleftharpoons \mathbf{ZnO} + \boldsymbol{H}_2 0 \quad (9)$$

2.4. Characterization of metal oxide nanoparticles

The properties of nanoparticles are affected by the synthetic method and parameters. In this study, the properties of the nanoparticles including the crystal structure, elemental composition, optical properties, morphology and the functional groups present were characterized using UV–Vis spectroscopy, X-ray diffraction and transmission electron microscopy analyses.

2.5. XRD analysis

The crystal structures for copper oxide and zinc oxide were respectively studied by an x-ray diffractometer (Empyrean, Malvern Panalytical, UK). The x-ray diffractometer carried out x-ray powder diffraction at a wavelength (λ) of 1.5418 Å within a 2θ range of 10° to 80°.

2.6. UV–Vis spectroscopy analysis

In this study the UV–Vis Spectrophotometer (Genesys 150 UV–Vis, ThermoFisher Scientific, USA) was adopted to obtain the UV–Vis spectrum of nanometal oxides. The measurement was done at a scanning

range of 200 nm–800 nm. A quartz cuvette filled with 1 ml aqueous suspension of respective nanometal oxide was analysed whiles using deionised water from Milli-Q as the blank solution for the measurement. The UV–Vis spectrum of nanoparticle is highly dependent on the particle size and shape which are determined by the fabrication method and the optimized parameters in the technique.

2.7. Transmission electron microscope (TEM) analysis of nanoparticles

TEM (JEOL 2010, JEOL Ltd., USA) was used to observe the morphologies of the synthesised nanoparticles. A minute sample of the synthesised particles were re-dispersed in an appropriate amount of water. The aqueous suspension was sonicated to overcome agglomeration resulting from drying the particles. A few drops of one to two of the sonicated suspension was immobilized on a carbon grid. The immobilized particles were evaporated and observed with TEM after it had dried.

2.8. FTIR analysis of metal oxide nanoparticles

A minute quantity of fine CuO and ZnO powders were separately placed on the clean infrared transparent surface of the FTIR instrument. The infrared scan was performed within the range of 4000–400 cm^{-1}.

2.9. Antibacteria testing

The antibacteria applications of nanometal oxides were carried out under sterile conditions inside a laminar flow cabinet. All media cultures, pipette tips water and glassware used for the microbiology testing were sterilized by autoclaving (UMB220 Benchtop Autoclave, Astell, USA) at 121 °C for 15 min. *Escherichia Coli* (*e. coli*) which is a gram negative bacteria and the *staphylococcus aureus* (*s. aureus*), a gram positive bacteria were used for the antibacterial studies.

2.9.1. Disk diffusion assay

Disk diffusion assays were prepared by the Kirby Bauer method. In this method, aqueous stock solutions of CuO and ZnO were appropriately prepared. Serial dilutions were prepared from the stock solution to obtain varying concentrated solutions of the nanometal oxides. Filter papers of approximately 6 mm were inserted into each aqueous suspension of nanoparticles and allowed to completely soak briefly. Subsequently, Mueller Hinton agar (MHA) media culture was prepared by dissolving 38 g of MHA in one litter of deionised water. The solution was autoclaved for 15 min at 121 °C. Disk plates of about 9 cm diameter were filled with a quantity of the prepared MHA in a sterilized laminar flow chamber and allowed to solidify shortly. *E. coli* and *s. aureus* were plated onto the agar plates by streaking. The paper disks were placed on the agar plate using a sterilize forceps. The plates were incubated at 37 °C overnight. Zones of inhibition surrounding the filter disc as a result of antibacteria activity of the nanoparticles were observed and measured with a millimetre rule and the measurements recorded accordingly.

2.9.2. Bacteria growth kinetic assay

The bacteria growth kinetic assay was carried out to observe the periodic growth of bacteria in a liquid broth. In this approach, optical density (OD) of the prepared assay were measured at regular interval and the changed in optical density which corresponds to bacteria growth were recorded. The assay was prepared by pipetting 60 µl of broth into a 96 well plate. To this, 20 µl (20 µl) of bacteria (*E. coli or S. Aureus*) at a concentration of 0.5 MacFarlad standard were individually added. Various concentrations of nanoparticles (1 mg/ml, 0.5 mg/ml, 0.25 mg/ml, 0.1 mg/ml, and 0.05 mg/ml) of 20 µl were added and the inoculum incubated at 37 °C on an orbital shaker at 225 rpm. Optical density of inoculum was recorded by measuring with the UV–Vis spectroscopy (VarioSCAN microplate reader) at period intervals of 2 h.

The following contents were made for each bacteria: Broth media, broth media + Bacteria; and finally Broth media + Bactria + Nanometal oxides. Each bacteria species was subjected to different concentrations (1 mg/ml, 0.5 mg/ml, 0.25 mg/ml, 0.1 mg/ml, and 0.05 mg/ml) of nanometal oxides.

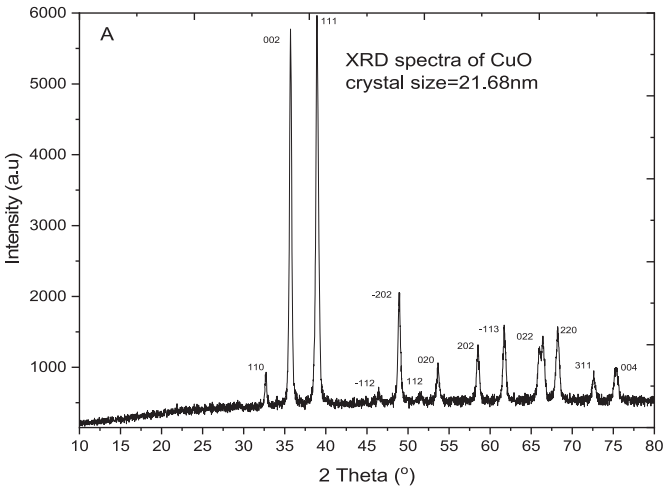

Fig. 1. XRD spectra pattern for copper oxide.

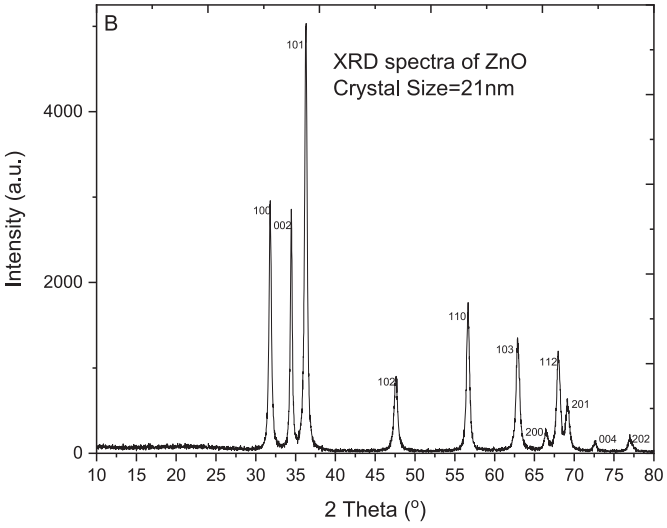

Fig. 2. XRD spectra pattern for Zinc Oxide.

3. Results and discussions

3.1. X-ray diffraction (XRD) analysis

The XRD patterns reveal that the as-synthesised nanometal oxides were fine and free of impurities (Fig. 1). There was no spectra peak relating to impurities that was found in any pattern. The diffraction patterns demonstrate sharp peaks as indication of the good crystallinity of the nano powders. The XRD patterns obtained for copper oxide are in exact agreement with the monoclinic phase of copper oxide. The spectra peaks had precise correlation with that of the monoclinic phase. Fig. 1 shows the XRD spectra pattern for copper oxide [22].

Fig. 2 illustrates the patterns for zinc oxide. The diffraction peaks of zinc oxide correctly matched the hexagonal wurtzite structure of zinc oxide. Scherer's equation was used to estimate the crystal sizes for copper oxide and zinc oxide as 21.68 nm and 21 nm respectively. The possible explanation to the difference between the crystal size recorded by XRD and the particle size recorded by TEM analysis is agglomeration.

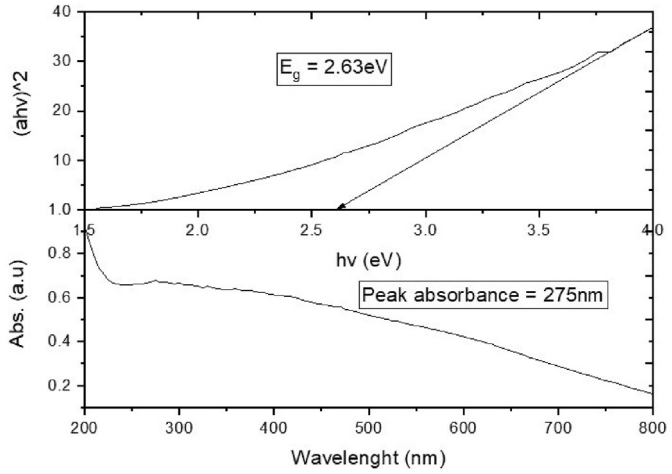

Fig. 3. UV–Vis spectrophotometer of Copper Oxide showing peak absorbance and its bandgap energy.

3.2. UV–Vis spectroscopy analysis of nanometal oxides

The UV–Vis spectrum of nanometal oxides showed peaks within the range of 200 nm to approximately 400 nm [23]. A UV–Vis analysis of the synthesised copper oxide and zinc oxide nanoparticles is shown in Fig. 1. The UV–Vis spectrum of absorbance (Abs.) versus wavelength showed peak absorbance at 275 nm which is an indication of electron transition from a valence band to a conduction band. This observation is attributed to the transition from the 2_p of oxygen to the 4_s of Cu^{2+} [22]. The broad range of the spectrum which ranges from the ultraviolet (UV) to visible light is typical of nanometal oxides. However, their highest peak occurred in the UV region [24]. The broad range also signifies that nanoparticles have a range of sizes and shape [25].

Copper oxide is a direct-band gap materials [26]. When a semiconductor such as nanometal oxide absorbs energy photon greater than its band gap energy, it causes the transfer of electrons from the valence band to the conduction band [27]. If the electron momentum in the transition process is conserved, then the material has a direct band gap [28]. The absorbance of the material corresponds to the wavelength and the energy band gap [29]. The absorption coefficient and the energy of direct-band gap materials are related by the Tauc's equation [28]. Hence the optical band gap of the spectrum is obtained by a plot of $(\boldsymbol{ahv})^2$ against $\boldsymbol{hv(eV)}$. Where 'a' is the absorption coefficient and 'h' and 'v' are respectively the plank's constant and the frequency of the waveform. The bandgap with respect to antibacteria activity provides information on the energy efficiency to the production of electrons leading to ionic species release which are considered toxic to cells [14]. The Tauc's relation in equation (10) describes a relationship between $(\boldsymbol{ahv})^2$ and the band gap energy $\boldsymbol{hv(eV)}$ in direct band gaps.

$$(\boldsymbol{ahv})^{\frac{1}{n}} \propto \boldsymbol{hv} - \boldsymbol{E_g} \tag{10}$$

where n is the order of refractive index. Thus, the x intercept of the waveform is the band gap energy.

The energy band gap of copper oxide nanoparticles was calculated to be 2.7 nm as indicated in Fig. 3. The band gap obtained is in agreement with previous works [27].

Zinc oxide nanoparticles shows a sharp peak at 355 nm (Fig. 4). This is due to the electron transfer across its band-gap. Electron transition occurs between the valence band and its conduction band. The 2d band of oxygen is the valence band of ZnO whiles the 3_d orbital of Zn^{2+} is the conduction band (S. S [7]. Implementing the same Tauc's equation for finding the band-gap energy. 3.22 eV was realised as the energy-band gap for the zinc oxide. A similar energy band-gap for has been reported for zinc oxide as a direct band gap with a wide band gap [30].

The semiconductor materials have the ability to promote electrons from the valence band to the conduction band with the help of photons from a light source. This creates electron-hole pairs. The electrons in the conduction band and the holes in the valence band interact with bacterial species to generate reactive oxygen species (ROS). ROS is responsible for the destruction of cell membranes and organelles. Thus, the antibacterial activity of nanoparticles is enabled by the generation of ROS activities.

A lower band gap means the metal oxide (nanoparticles) can obtain the necessary photon at lower energy wavelength to cause ROS activities. A higher band gap means the energy can be obtained in a higher energy. A lower energy can be the visible light which can be obtained from normal daylight and a higher energy may be ultraviolet light (UV) which can be obtained by extended aid. The UV–Vis spectrum of copper oxide and zinc oxide shows that copper oxide has lower energy band gap

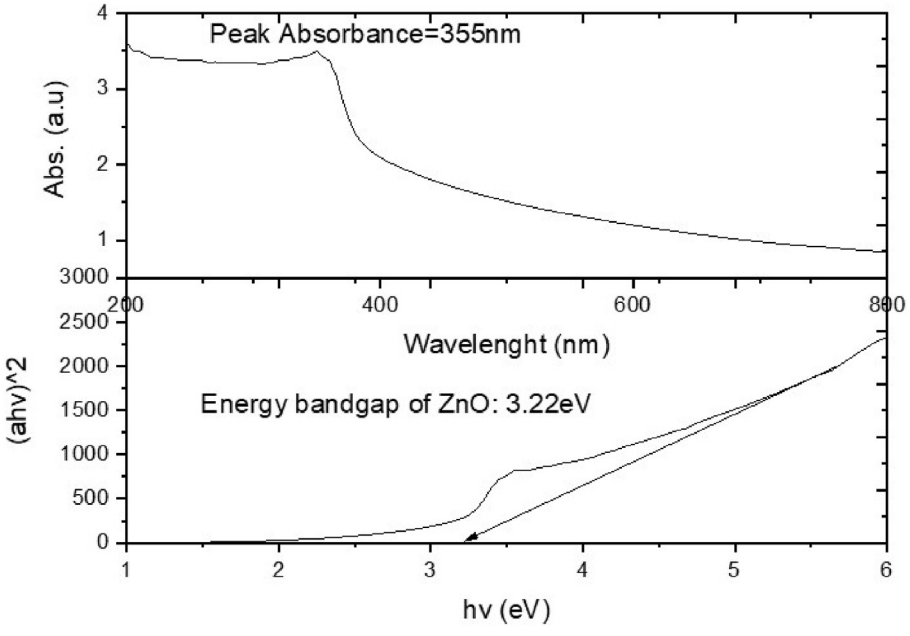

Fig. 4. UV–Vis spectrophotometer of Zinc Oxide showing peak absorbance and its bandgap energy.

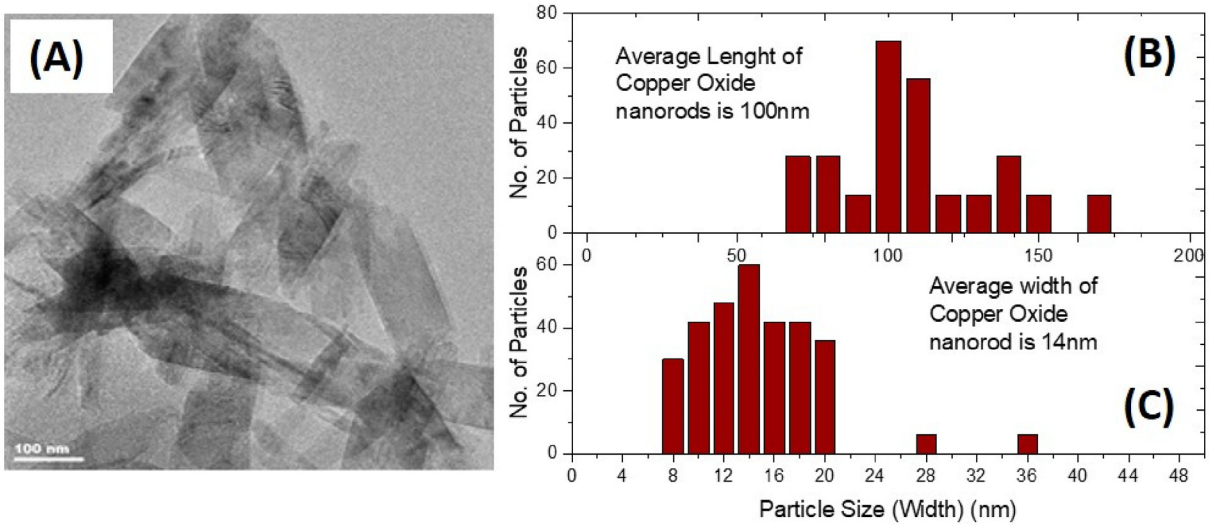

Fig. 5. (A) A TEM micrograph of copper oxide nanoparticles. (B) A histogram distribution of the length of the nanoparticles (C) A histogram showing the distribution in the width of the nanoparticles.

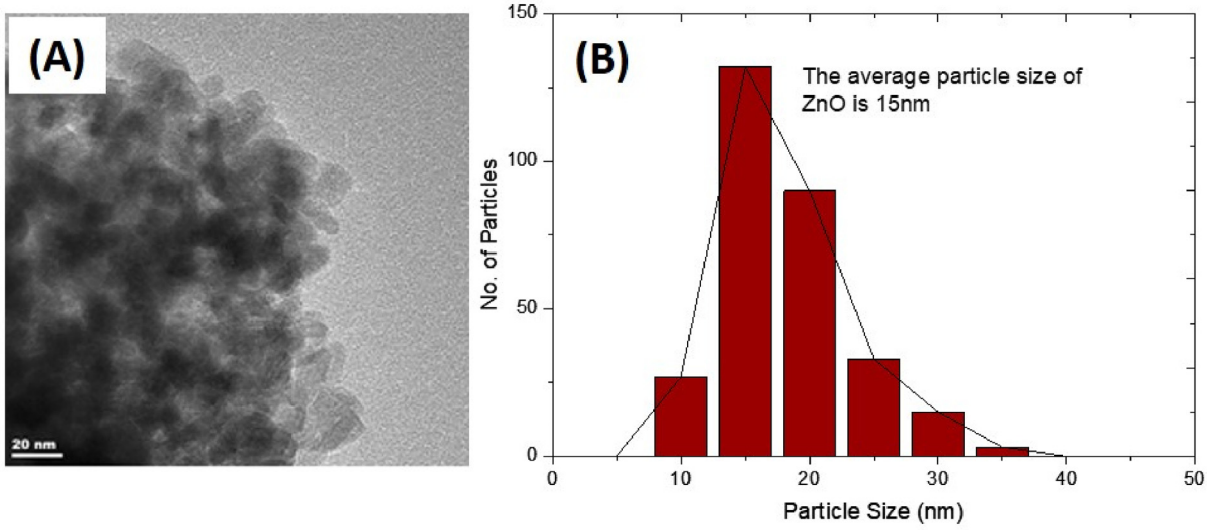

Fig. 6. (A) A TEM micrograph of zinc oxide nanoparticles. (B) A histogram distribution of the size of the zinc oxide nanoparticles.

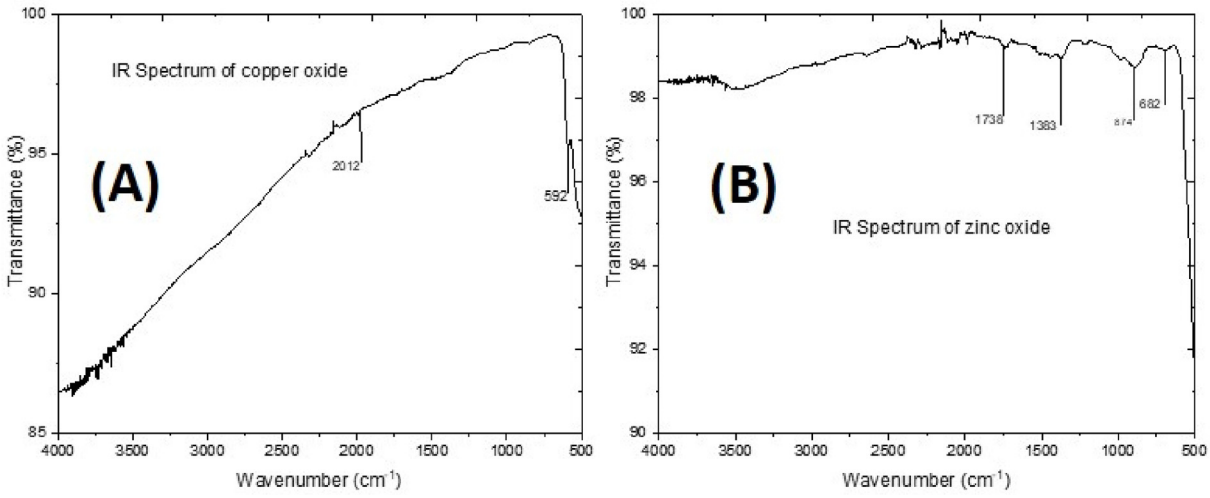

Fig. 7. Infrared spectra analysis of (A) Copper oxide and (B) Zinc oxide nanoparticles.

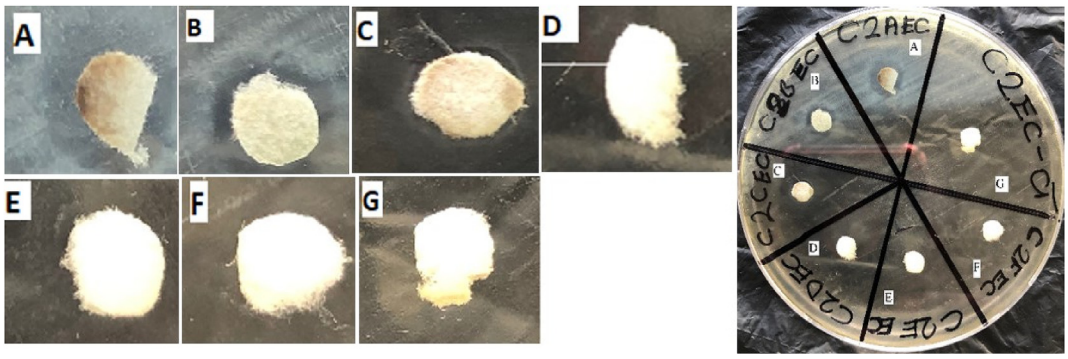

Fig. 8. Antibacteria activity of copper oxide on *e. coli.*

relative to zinc oxide. This means that copper oxide in the presence of visible light can more easily produce electrons in solution than zinc oxide. Thus copper oxide in such a condition is expected to result in more ROS activity hence higher antibacteria activity as compared to zinc oxide.

3.3. Transmission electron microscope (TEM) analysis of nanoparticles

The TEM micrographs reveal that the wet-chemical aqueous precipitation synthesis method produced copper oxide nanorods. As demonstrated in Fig. 5, the synthesised nanoparticles agglomerated in bundles or clusters of nanorods. The nanorods occurred in lengths varying from 70 nm to 170 nm. The average length of the nanorods was observed to be 100 nm. The width of the nanorods was found to range from 8 nm to 36 nm with 14 nm as the average width of the nanorods.

The TEM micrograph of zinc oxide nanoparticles is shown in Fig. 6. Unlike copper oxide, wet-chemical aqueous precipitation synthesis of zinc oxide did assume a more spherical shape. The particles were also however more broadly distributed in size. The size analysed by Image J showed that it ranged from 10 nm to 35 nm. The average size was 15 nm. Wet chemical aqueous precipitation synthesis of nanometal oxides has revealed that whiles it produces nanorod copper oxides, it however creates zinc oxides that are predominantly spherically shapes. The zinc oxide produced are more widely distributed in size as compared to the copper oxide nanorods.

3.4. FTIR analysis of metal oxide nanoparticles

The infrared spectra of copper oxide nanorods is shown in Fig. 5a. The peak observed at 596 cm^{-1} is a band associated with the stretching vibration of Cu–O bonds. The absorption bands within 1350 cm^{-1} and 1650 cm^{-1} are indications of atmospheric CO_2. Spectra bands occurring between 2800 and 3500 cm^{-1} corresponds to O–H bonds. O–H bonds

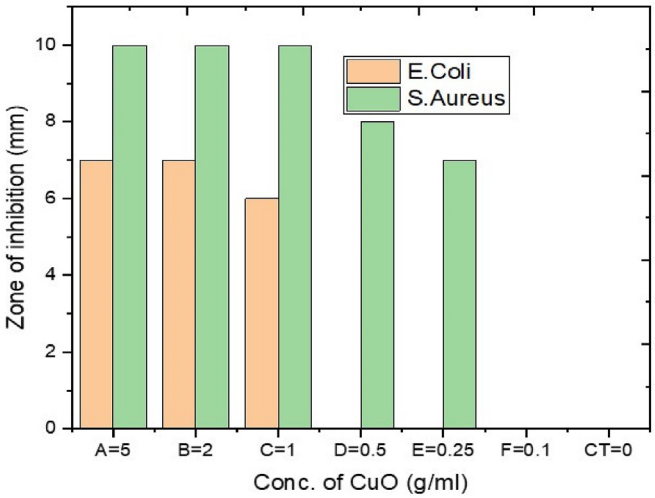

Fig. 10. A comparative assessment of the activity of copper oxide on *e. coli* and *s. aureus*.

with very low bands are due to the minute presence of a moisture content. The FTIR in Fig. 7 confirms that copper oxide was synthesised and confirmed by the presence of Cu–O bond. The FTIR spectra analysis of zinc oxide is shown in Fig. 5b. The absorption band at 863 cm^{-1} is an indication of Zn–O vibration.

The FTIR spectra shows that there were no surfactant present on the surface of both nanoparticle samples. This can be deduced from the absence of significant amount of any organic species on the surface of nanoparticles. Hence surfactant free nanoparticles were synthesised which is important to study the original contribution of either nanoparticles in antibacteria activity.

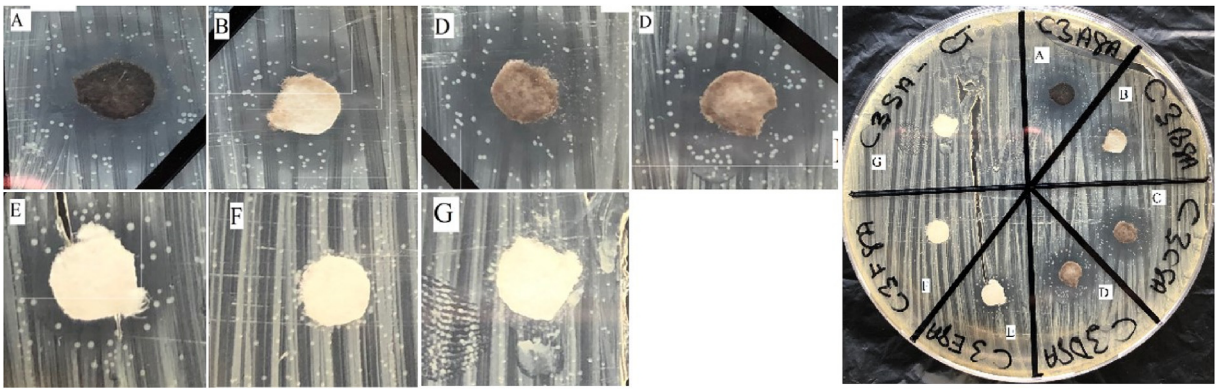

Fig. 9. Antibacteria activity of copper oxide on S. Aureus.

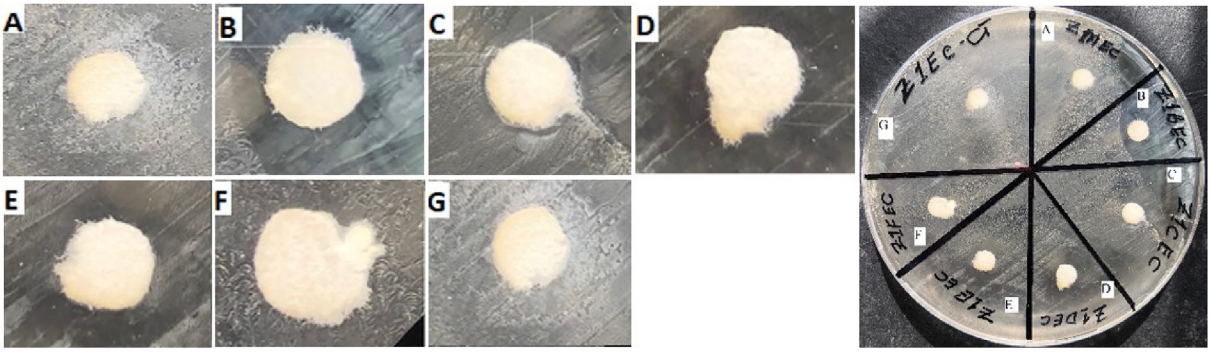

Fig. 11. Antibacteria activity of zinc oxide on *e. coli*.

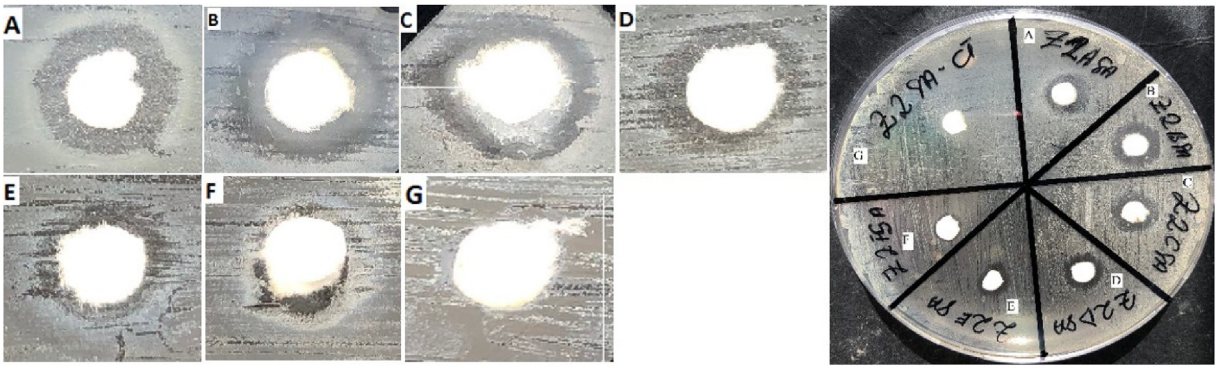

Fig. 12. Antibacteria activity of zinc oxide nanoparticles on *s. aureus*.

3.5. Antibacteria study of nanometal oxides against bacteria species

3.5.1. Disk diffusion studies

The Kirby Bauer Disk diffusion method was employed to investigate antibacteria activity of nanometal oxides on bacteria species. Aqueous suspension of nanometal oxides ranging from 5 mg/ml to 0.01 mg/ml were tested on *e. coli* and *s. aureus* which represent gram positive and gram negative bacteria species. Nanometal oxides demonstrated varying activity against the gram negative and gram positive bacteria species.

Fig. 8 indicates that copper oxide showed varying activity on *e. coli* which is a gram negative bacteria.

The activity depended on the concentration of copper oxide. Copper oxide concentrations of 5 mg/ml and 2 mg/ml showed significant activity on *e. coli*. Copper oxide concentrations of 1 mg/ml had a marginal activity on *E. coli* whiles concentrations lower than 1 mg/ml had no significant activity on the *e. coli*. Copper oxide however showed higher activity on *s. aureus*. Copper oxide concentrations from 5 mg/ml to 0.25 g/ml showed activity on *s. aureus* as demonstrated in Fig. 9.

Fig. 10 shows a histogram comparing the activity of copper oxide on *e. coli* and *s. aureus*.

E. coli was more resistive to the antibacteria activity of copper oxide as compare to *s. aureus* Zinc oxide nanoparticles was similarly tested on *e. coli* and *s. aureus*. Fig. 11 reveals the activity of zinc oxide nanoparticles on *e. coli*. The results demonstrates that zinc oxide had no effect on *e. coli*. All the concentrations of zinc oxide from 5 mg/ml to 0.01 mg/ml showed no activity against *e. coli*. Thus, all the various concentrations of zinc oxide nanoparticles recorded no zone of inhibition when tested on *e. coli*.

Zinc oxide nanoparticles were likewise tested on S. Aureus. Unlike its performance on *e. coli*, zinc oxide nanoparticles showed effect on *s. aureus*. The various concentrations of nanoparticles ranging from 5 mg/ml to 0.01 mg/ml showed an effect on *s. aureus*. The effect shown on *s. aureus* increased with increasing concentration. Fig. 12 shows the activity of zinc oxide on *s. aureus*.

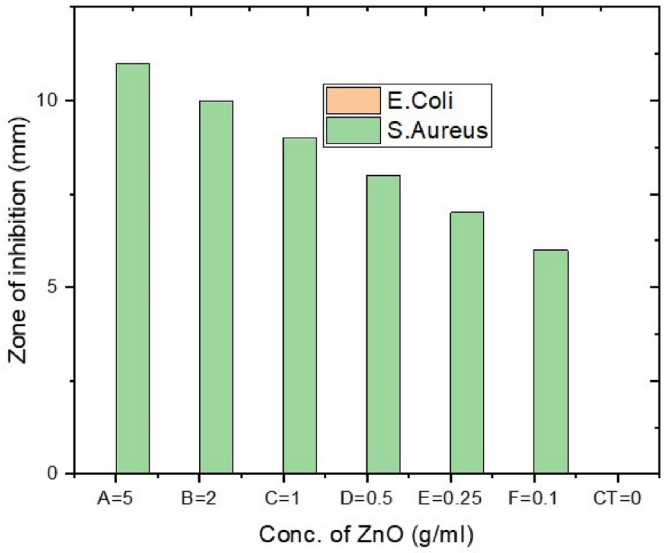

Fig. 13. Histogram showing the relative activity of zinc oxide on *e. coli* and *s. aureus*.

Whiles zinc oxide showed activity against S, Aureus it was ineffective against *e. coli*. Fig. 13 is a histogram of the activity of zinc oxide on *e. coli* and *s. aureus*.

The Kirby Bauer disk diffusion method of antibacteria testing revealed that *e. coli* strain ATCC25923 is resistive to nanometal oxides of zinc oxide. Copper oxide nanoparticles were slightly effective against the nanoparticles. Meanwhile *s. aureus* strain ATCC25923 tested with the same sets of nanoparticles indicated that the nanoparticles were efficient in resulting in cell death in the order of increasing concentration. Fig. 14

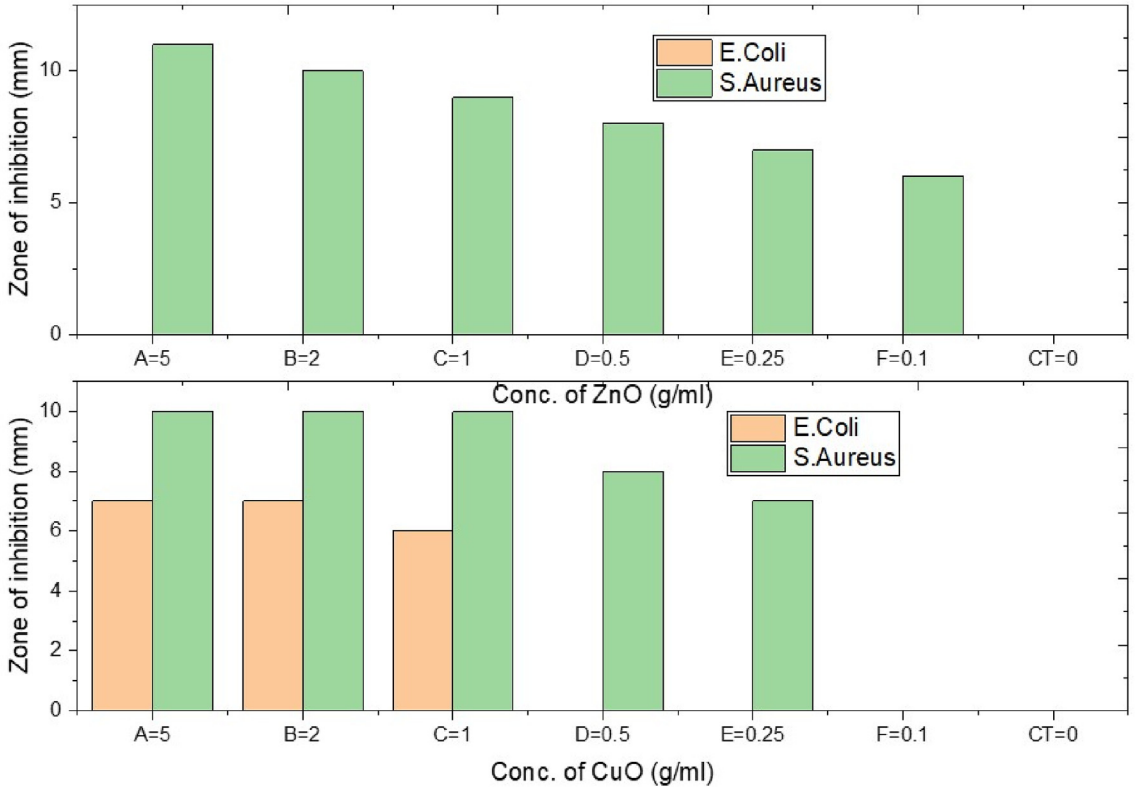

Fig. 14. A histogram showing the comparison of the antibacteria activity of copper oxide and zinc oxide on *e. coli* and *s. aureus*.

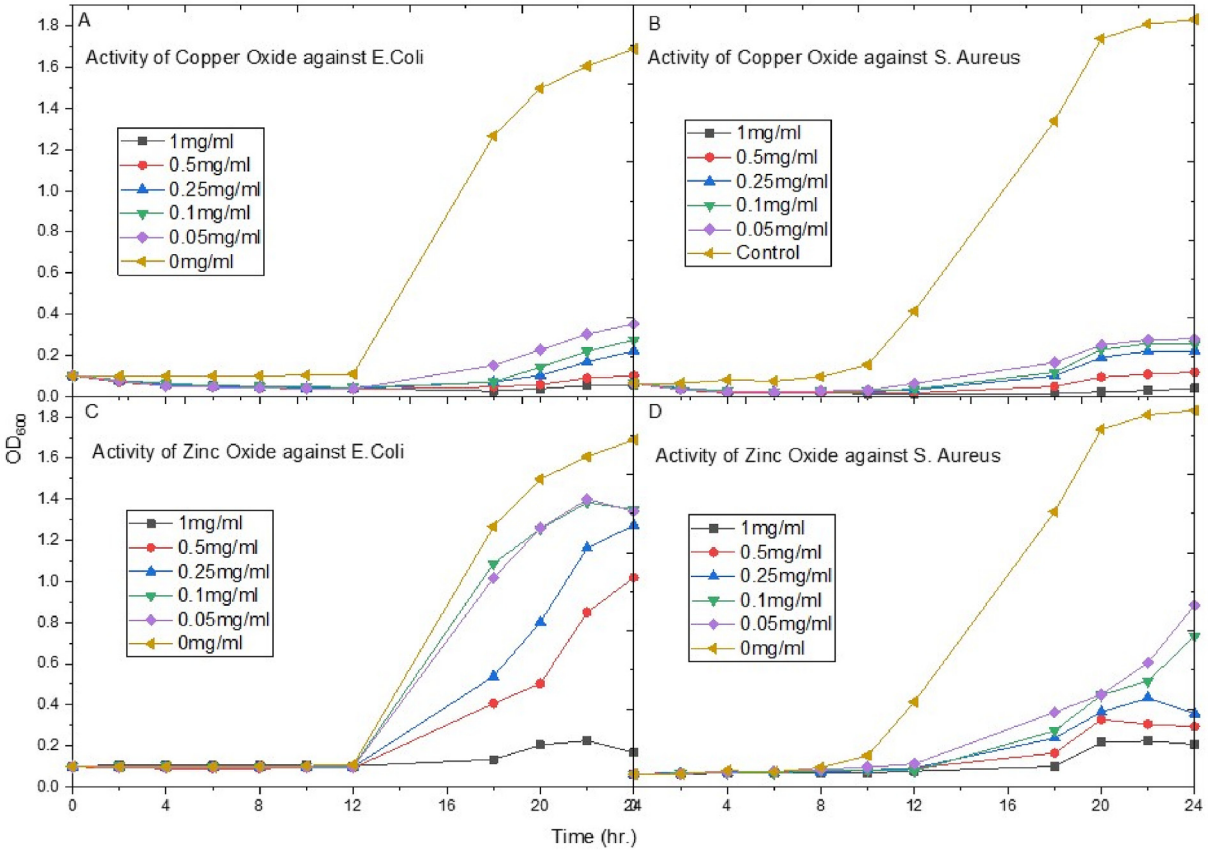

Fig. 15. Dynamic growth kinetic study of the activity of: (A) Copper Oxide against *e. coli* (B) Copper Oxide against *s. aureus* (C) Zinc Oxide AGAINST *E. coli* and (D) Zinc Oxide against *S. aureus*.

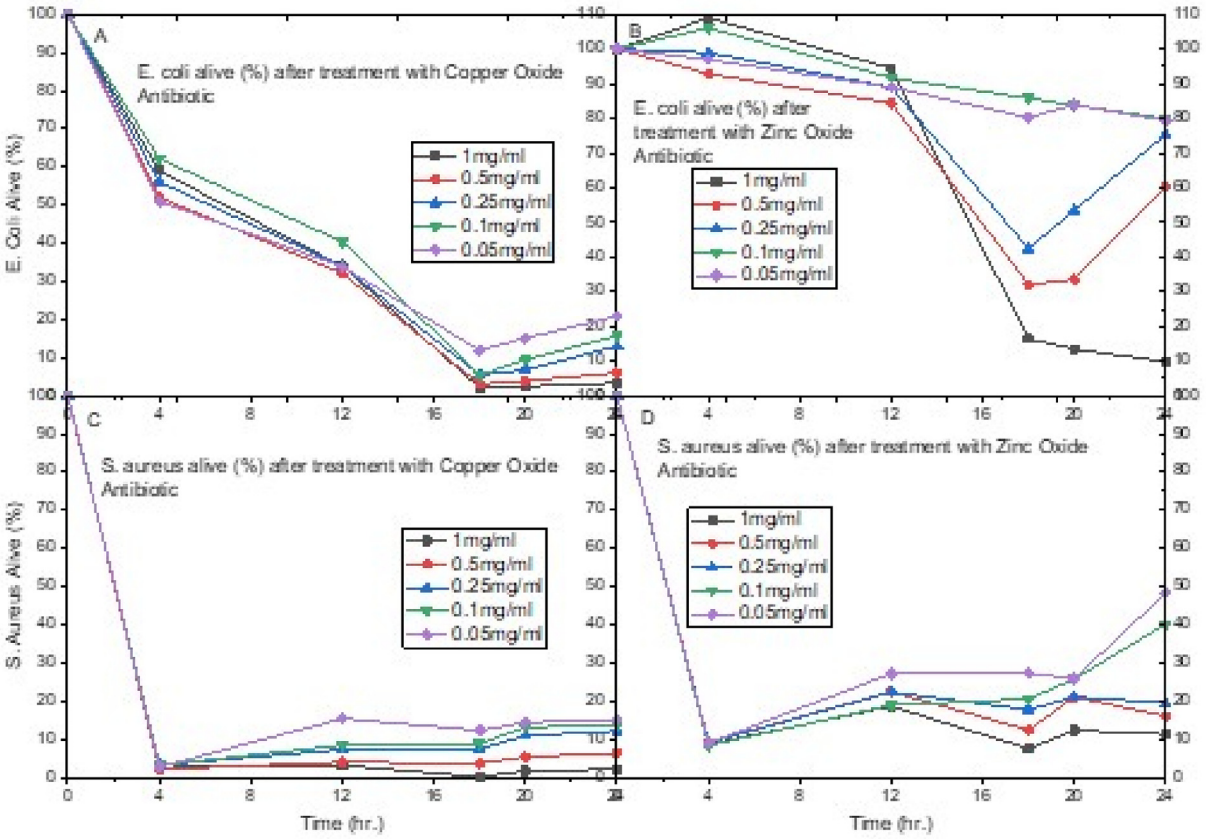

Fig. 16. Dynamic growth kinetic study on (A) *e. coli* alive (%) after treatment with copper oxide (B) *e. coli* alive (%) after treatment with zinc oxide (C) *S. aureus* alive (%) after treatment with copper oxide (D) *s. aureus* alive (%) after treatment with zinc oxide.

compares the efficiency of zinc oxide and copper oxide nanoparticles against *e. coli* and *s. aureus*.

3.5.2. *Bacteria growth kinetic study*

To understand the kinetics of anti-bacterial activity, liquid broth assay provides a more idle method. Liquid broth assay which is also popularly called the broth microdilution examines changes in the growth of bacteria in a broth (liquid) assay by measuring its optical density. The optical density of the assay provides an estimation of the amount of bacteria cells present in the assay. Spectrophotometer measure optical density of bacteria cells by recording the concentration of the cells at an absorbance of 600 nm. Meanwhile, nanometal oxides may have absorbance within the range of 600 nm which is excluded from the analysis. The antibacteria kinetics studies provides information on the rate of activity of metal oxides on bacteria species.

The growth kinetics studies began with the same number of bacteria cells for both gram positive and gram-negative bacteria. $6*10^6$ CFU was used as the starting amount of bacteria. Corresponding changes in the initial bacteria density was measured by noting its corresponding changes in optical density at 600 nm. The bacteria growth dynamics studies was with and without the presence of nanometal oxides. Assays without nanometal oxides was used as a reference for antibacteria studies. Thus the dynamic bacteria growth depended on the antibacteria metal oxides. Varying concentrations (1 mg/ml, 0.5 mg/ml, 0.25 mg/ml, 0.1 mg/ml, 0.05 mg/ml) of both copper oxide and zinc oxide were applied on both the gram positive and gram negative bacteria. The bacteria growth kinetic study is shown in Fig. 15.

Copper oxide showed relatively higher activity against both *e. coli* and *s. aureus*. The activity of both copper oxide and zinc oxide was more effective against *S. aureus* than *E. coli*. A similar results have been reported by other authors on the relative efficiency of nanoparticles against gram positive bacteria such as *s. aureus* than gram negative bacteria such as *e. coli* [31]. Although gram positive bacteria have comparatively thicker cell wall which is expected to make them more resistive to nanoparticles, recent works hypothesised that the gram negative bacteria of *e. coli* possess flagellum which could cause the agglomeration of nanoparticles [32]. The agglomeration of nanoparticles significantly reduces their toxic effect [33]. The results obtained in the optical density test agrees with the results of the disk diffusion test. In the disk diffusion test, copper oxide nanoparticles again showed enhanced activity in both bacteria species than zinc oxide.

Fig. 16 demonstrates the amount of bacteria cells present in the inoculum with respect to time after treatment with the respective nanoparticles at their varying concentrations. It can be realised from the figure that in the case of *e. coli*, the dynamic kinetic growth curve has a gradual slope. It reaches its minimum point after a prolong time of treatment. This means that the antibiotic effect of the nanoparticles takes a considerable length of time to result in the death of *e. coli* cells. Thus, *e. coli* cells are tolerable to the antibiotic effect of the nanoparticles for a considerable length of time. It can also be deduced from the *e. coli* (%) versus Time (hr) plot that copper oxide had the most effect on *e. coli* as compared to Zinc oxide. More *e. coli* cells remained alive in the respective inoculum treated with nanoparticle concentrations of zinc oxide as compared to those of copper oxide. The *e coli* cells were thus more resistive to zinc oxide nanoparticles than copper oxide nanoparticles (see Fig. 17).

In the case of *s. aureus*, the *s. aureus* alive (%) versus Time (hr) plot has a very sharp slope. That is *s. aureus* cells were very susceptible to both nanoparticles. Similarly, it is also observed that copper oxide nanoparticles were comparably more toxic to the *s. aureus* cells hence relatively less amount of *s. aureus* cells remained alive with respect to time.

A similar observation was made in the disk diffusion test. Copper

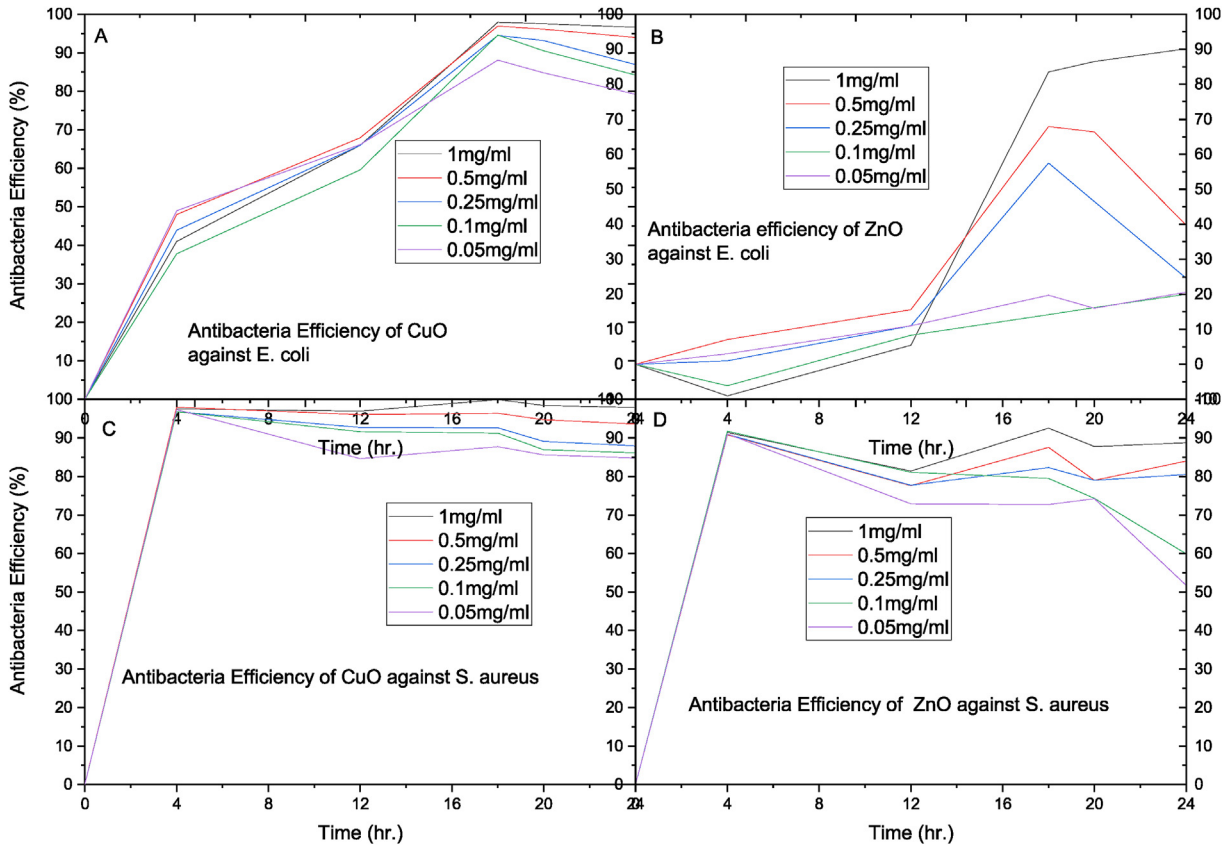

Fig. 17. Dynamic growth kinetic study on (A) Antibacteria efficiency of copper oxide against *e. coli* (B) Antibacteria efficiency of zinc oxide against *e. coli* (C) Antibacteria efficiency of copper oxide against *s. aureus* (D) Antibacteria efficiency of zinc oxide against *s. aureus*.

oxide nanoparticles were comparably more effective on both *e. coli* and *s. aureus* as compared to zinc oxide.

Fig. 16 shows the efficiencies of the respective nanoparticles on the different bacteria species. The efficiencies of the nanoparticles were each observed to be dependent on the concentration of the nanoparticle used for bacteria treatment. The efficiency in the case of each nanoparticle increased with increasing the nanoparticle concentration. A similar observation is common among experimental studies in drug-pathogen relationships. In the case of the disk diffusion, a similar pattern of antibiotic activity was observed. The effect of the disk carrying antibiotic nanoparticles was dependent on the concentration of nanoparticle suspension in which it was immersed or dipped. The higher the concentration the higher the amount of nanoparticle or nanoparticle ions immobilized on the disk for antibacteria activity.

According to Fig. 16, copper oxide nanoparticles at the concentration of 1 mg/ml could achieve antibacteria efficiency of approximately 99% against both *e. coli* and *s. aureus.* Zinc oxide achieved 90% and 89% respectively for *e. coli* and *s. aureus* at the same concentration. Hence, coper oxide demonstrated higher antibacteria activity against both *e. coli* and *s. aureus* as compared to zinc oxide.

4. Conclusion and future work

In this study, facile method was used to achieve the complete synthesis of ultra-fine nanometal oxide particles. The synthesis method which was fast, inexpensive and easy to carry out was also easy to separate from suspension for preparation for characterization studies. The characterization results showed that the easily synthesised nanometal oxides were void of impurities and achieved high degree of crystalline nature with diffraction peaks well indexed to known and hypothesised patterns. The facile synthesised particles achieved optical properties conforming to their existing kinds with particles size below 100 nm which categorises them as nanoparticles. The synthesised particles were further characterized to free of surfactant hence their antibacteria activity would be unaided by organic species which could also possess antibacteria activity. The antibacteria activity of the nanometal oxides on gram negative bacteria and gram positive which were respectively *E. coli* and *S. aureus* showed that both nanometal oxides of copper oxide and zinc oxide could inhibit bacteria activity dependent on their concentration. The antibacteria activity increased directly proportional to their concentration. However, this study revelation demonstrates two different but complementing methods of antibacteria testing which are the disk diffusion and the optical density test that copper oxide possessed a comparatively higher antibacteria on both gram negative bacteria which is *e. coli* and gram positive bacteria which is *s. aureus*. The results is useful for the synthesis, characterization and the relative antibacteria efficiencies of two of the most popular metal oxide antibacteria agents. Further studies may be carried into the impart of different synthesis methods on the properties and the effects of these two widely considered metal oxide nanometal oxides.

CRediT authorship contribution statement

R.B. Asamoah: Investigation, Writing - original draft. **A. Yaya:** Conceptualization, Resources, Methodology, Supervision. **B. Mensah:** Validation, Writing - review & editing. **P. Nbalayim:** Validation, Writing - review & editing. **V. Apalangya:** Writing - review & editing, Visualization. **Y.D. Bensah:** Validation, Writing - review & editing. **L.N.W. Damoah:** Formal analysis, Writing - review & editing. **B. Agyei-Tuffour:** Validation, Writing - review & editing. **D. Dodoo-Arhin:** Validation, Writing - review & editing. **E. Annan:** Supervision, Conceptualization, Writing - review & editing.

Acknowledgement

This research was supported by Building a New Generation of Academics in Africa" (BaNGA-Africa) project at the University of Ghana, Legon. ORID project number URF/10/ILG-083/2016–2017 though the Office Research Innovation and Development (ORID) is partial support is also acknowledged.

References

[1] P. Pandey, et al., Antimicrobial Properties of CuO Nanorods and Multi-Armed Nanoparticles against B . Anthracis Vegetative Cells and Endospores, 2014, pp. 789–800, https://doi.org/10.3762/bjnano.5.91.
[2] Cdc, C. for D. C, Diarrhea: common illness, global killer, Fact Sheet (2018) 1–4. Available at: https://www.cdc.gov/healthywater/pdf/global/programs/globaldiarrhea508c.pdf%0Ahttps://www.cdc.gov/healthywater/global/diarrhea-burden.html.
[3] S. Kar, et al., 'Biochimica et Biophysica Acta Synthesis and characterization of Cu/Ag nanoparticle loaded mullite nanocomposite system : a potential candidate for antimicrobial and therapeutic applications', BBA - Gen. Sub. Els.B.V. 1840 (11) (2014) 3264–3276, https://doi.org/10.1016/j.bbagen.2014.05.012.
[4] G. Franci, et al., Silver nanoparticles as potential antibacterial agents, Molecules 20 (5) (2015) 8856–8874, https://doi.org/10.3390/molecules20058856.
[5] R. Foldbjerg, et al., Toxicology Research', (2010, 2015, pp. 563–575, https://doi.org/10.1039/c4tx00110a.
[6] A. Ivask, et al., Toxicity of Ag , CuO and ZnO Nanoparticles to Selected Environmentally Relevant Test Organisms and Mammalian Cells in Vitro : a Critical Review, 2013, pp. 1181–1200, https://doi.org/10.1007/s00204-013-1079-4.
[7] A. Kumar, et al., Facile synthesis of size-tunable copper and copper oxide nanoparticles using reverse microemulsions, RSC Adv. 3 (15) (2013) 5015, https://doi.org/10.1039/c3ra23455j.
[8] S. Ahmed, et al., 'REVIEW A review on plants extract mediated synthesis of silver nanoparticles for antimicrobial applications : a green expertise' 7, Cairo University, 2016, pp. 17–28, https://doi.org/10.1016/j.jare.2015.02.007. J. Adv. Res.1.
[9] M. Sahooli, S. Sabbaghi, R. Saboori, Synthesis and Characterization of Mono Sized CuO Nanoparticles', Materials Letters, vol. 81, Elsevier B.V., 2012, pp. 169–172, https://doi.org/10.1016/j.matlet.2012.04.148.
[10] H. Palza, Antimicrobial Polymers with Metal Nanoparticles, 2015, pp. 2099–2116, https://doi.org/10.3390/ijms16012099.
[11] S. Agnihotri, Soumyo Mukherji, Suparna Mukherji, 'Size-controlled silver nanoparticles synthesized over the range 5–100 nm using the same protocol and their antibacterial efficacy', RSC Adv. 4 (8) (2014) 3974–3983, https://doi.org/10.1039/C3RA44507K.
[12] A. Pietro Reverberi, et al., Synthesis of Copper Nanoparticles in Ethylene Glycol by Chemical Reduction with Vanadium (+ 2) Salts, 2016, pp. 1–11, https://doi.org/10.3390/ma9100809.
[13] K. Nakata, T. Tsuchido, Y. Matsumura, Antimicrobial Cationic Surfactant , Cetyltrimethylammonium Bromide , Induces Superoxide Stress in Escherichia coli Cells, 2010, pp. 568–579, https://doi.org/10.1111/j.1365-2672.2010.04912.x.
[14] Z. Xiu, et al., Negligible Particle-Speci Fi C Antibacterial Activity of Silver Nanoparticles, 2012, pp. 10–14.
[15] Q.L. Feng, et al., A Mechanistic Study of the Antibacterial Effect of Silver Ions on Escherichia coli and Staphylococcus aureus, 2000.
[16] K. Chandraker, et al., Radical scavenging efficacy of thiol capped silver nanoparticles, J. Chem. Sci. 127 (12) (2015) 2183–2191, https://doi.org/10.1007/s12039-015-0968-x.
[17] A. El-Trass, et al., CuO nanoparticles: synthesis, characterization, optical properties and interaction with amino acids, Appl. Surface Sci. Els. B.V. 258 (7) (2012) 2997–3001, https://doi.org/10.1016/j.apsusc.2011.11.025.
[18] M.J. Hajipour, et al., Antibacterial properties of nanoparticles, Trends Biotechnol. Els. Ltd. 30 (10) (2012) 499–511, https://doi.org/10.1016/j.tibtech.2012.06.004.
[19] N. Topnani, S. Kushwaha, T. Athar, Wet synthesis of copper oxide nanopowder, Int. J. Green Nanotechnol. Mater. Sci. Eng. 1 (2) (2010), https://doi.org/10.1080/19430840903430220.
[20] J. Zhang, Silver-coated Zinc Oxide Nanoantibacterial Synthesis and Antibacterial Activity Characterization J, V3–95', 2011, pp. 94–98 (Iceoe).
[21] J. Konieczny, Z. Rdzawski, Antibacterial properties of copper and its alloys, Arch. Mater. Sci. Eng. 56 (7) (2012) 53–60.
[22] M. Dahrul, H. Alatas, Irzaman, Preparation and Optical Properties Study of CuO Thin Film as Applied Solar Cell on LAPAN-IPB Satellite', Procedia Environmental Sciences, vol. 33, Elsevier B.V., 2016, pp. 661–667, https://doi.org/10.1016/j.proenv.2016.03.121.
[23] C. A. De Caro, UV/VIS Spectrophotometry, Mettler Toledo, 2017, pp. 4–14. November.
[24] K. Mondal, Recent Advances in the Synthesis of Metal Oxide Nanofibers and Their Environmental Remediation Applications, 2017, pp. 1–29, https://doi.org/10.3390/inventions2020009.
[25] K.S. Khashan, M.S. Jabir, F.A. Abdulameer, Preparation and characterization of copper oxide nanoparticles decorated carbon nanoparticles using laser ablation in liquid, J. Phys. Conf. 1003 (1) (2018), https://doi.org/10.1088/1742-6596/1003/1/012100.
[26] F.K. Mugwanga, et al., Optical characterization of Copper Oxide thin films prepared by reactive dc magnetron sputtering for solar cell applications, Int. J. Thin Films Sci. Technol. 2 (1) (2013) 12–24, https://doi.org/10.1016/S0042-207X(00)00151-2.
[27] Y. Wang, et al., Electronic structures of C u2 O, C u4 O3, and CuO: a joint experimental and theoretical study, Phys. Rev. B 94 (24) (2016), https://doi.org/10.1103/PhysRevB.94.245418.
[28] S. Das, T.L. Alford, Structural and optical properties of Ag-doped copper oxide thin films on polyethylene napthalate substrate prepared by low temperature microwave annealing, J. Appl. Phys. 113 (24) (2013), https://doi.org/10.1063/1.4812584.
[29] H. Kumar, R. Rani, Structural and optical characterization of ZnO nanoparticles synthesized by microemulsion route, Int. Lett. Chem. Phys. Astron. 19 (2013) 26–36, https://doi.org/10.18052/www.scipress.com/ilcpa.19.26.
[30] G. Varughese, P. Jithin, K. Usha, Determination of optical band gap energy of wurtzite ZnO: Ce nanocrystallites, Phys. Sci. Int. J. 5 (2) (2015) 146–154, https://doi.org/10.9734/psij/2015/14151.
[31] W.K. Jung, et al., Antibacterial Activity and Mechanism of Action of the Silver Ion in Staphylococcus aureus and Escherichia coli, vol. 74, 2008, pp. 2171–2178, https://doi.org/10.1128/AEM.02001-07, 7.
[32] M.F. Salas Orozco, et al., Molecular mechanisms of bacterial resistance to metal and metal oxide nanoparticles, Int. J. Mol. Sci. 20 (11) (2019), https://doi.org/10.3390/ijms20112808.
[33] N.R.N. Roselina, A. Azizan, 'Ni Nanoparticles : Study of Particles Formation and Agglomeration', vol. 41, 2012, pp. 1620–1626, https://doi.org/10.1016/j.proeng.2012.07.359.